Title

Subretinal implantation of a monolayer of human embryonic stem cell-derived retinal pigment epithelium: a feasibility and safety study in Yucatán minipigs.

Journal

Graefe's archive for clinical and experimental ophthalmology = Albrecht von Graefes Archiv fur klinische und experimentelle Ophthalmologie, 254(8)

ISSN

0721-832X

Authors

Koss, Michael J
Falabella, Paulo
Stefanini, Francisco R
et al.

Publication Date

2016-08-01

DOI

10.1007/s00417-016-3386-y

Peer reviewed

Graefes Arch Clin Exp Ophthalmol (2016) 254:1553–1565
DOI 10.1007/s00417-016-3386-y

BASIC SCIENCE

Subretinal implantation of a monolayer of human embryonic stem cell-derived retinal pigment epithelium: a feasibility and safety study in Yucatán minipigs

Michael J. Koss[1,2] · Paulo Falabella[2] · Francisco R. Stefanini[3] · Marcel Pfister[2] · Biju B. Thomas[2] · Amir H. Kashani[2] · Rodrigo Brant[3] · Danhong Zhu[2,4] · Dennis O. Clegg[5] · David R. Hinton[2,4] · Mark S. Humayun[2,6]

Received: 16 December 2015 / Revised: 23 March 2016 / Accepted: 11 May 2016 / Published online: 22 June 2016

Abstract
Purpose A subretinal implant termed CPCB-RPE1 is currently being developed to surgically replace dystrophic RPE in patients with dry age-related macular degeneration (AMD) and severe vision loss. CPCB-RPE1 is composed of a terminally differentiated, polarized human embryonic stem cell-derived RPE (hESC-RPE) monolayer pre-grown on a biocompatible, mesh-supported submicron parylene C membrane. The objective of the present delivery study was to assess the feasibility and 1-month safety of CPCB-RPE1 implantation in Yucatán minipigs, whose eyes are similar to human eyes in size and gross retinal anatomy.
Methods This was a prospective, partially blinded, randomized study in 14 normal-sighted female Yucatán minipigs (aged 2 months, weighing 24–35 kg). Surgeons were blinded to the randomization codes and postoperative and post-mortem assessments were performed in a blinded manner. Eleven minipigs received CPCB-RPE1 while three control minipigs underwent sham surgery that generated subretinal blebs. All animals except two sham controls received combined local (Ozurdex™ dexamethasone intravitreal implant) and systemic (tacrolimus) immunosuppression or local immunosuppression alone. Correct placement of the CPCB-RPE1 implant was assessed by in vivo optical coherence tomography and post-mortem histology. hESC-RPE cells were identified using immunohistochemistry staining for TRA-1-85 (a human marker) and RPE65 (an RPE marker). As the study results of primary interest were nonnumerical no statistical analysis or tests were conducted.
Results CPCB-RPE1 implants were reliably placed, without implant breakage, in the subretinal space of the minipig eye using surgical techniques similar to those that would be used in humans. Histologically, hESC-RPE cells were found to survive as an intact monolayer for 1 month based on immunohistochemistry staining for TRA-1-85 and RPE65.
Conclusions Although inconclusive regarding the necessity or benefit of systemic or local immunosuppression, our study demonstrates the feasibility and safety of CPCB-RPE1 subretinal implantation in a comparable animal model and provides an encouraging starting point for human studies.

Keywords Human embryonic stem cells · Retinal pigment epithelium · Macular degeneration · Preclinical trial · Animal model

✉ Michael J. Koss
michael.koss@me.com

[1] Department of Ophthalmology, University of Heidelberg, Im Neuenheimer Feld 400, 69120 Heidelberg, Germany

[2] USC Eye Institute, University of Southern California, 1450 San Pablo Street, Los Angeles, CA 90033-4682, USA

[3] Department of Ophthalmology, Federal University of São Paulo UNIFESP, Rua Botucatu 821, 04023-062 São Paulo, Brazil

[4] Department of Pathology, Keck School of Medicine, University of Southern California, 1450 San Pablo Street, Los Angeles, CA 90033-4682, USA

[5] Department of Molecular, Cellular, and Developmental Biology, University of California, Santa Barbara, Santa Barbara, CA 93106-9625, USA

[6] Institute of Biomedical Therapeutics, University of Southern California, 1450 San Pablo Street, Los Angeles, CA 90033-4682, USA

Introduction

Age-related macular degeneration (AMD) is the leading cause of blindness among the elderly worldwide and is characterized

by the degeneration of retinal pigment epithelium (RPE) and photoreceptor cells in the central region of the retina, leading to progressive and significant central vision loss [1]. In the era before the advent of vascular endothelial growth factor-targeted treatment, surgical pioneers subretinally transplanted autologous adult [2] or allogeneic homologous fetal RPE in wet and dry human AMD but rejection rates were high despite better outcomes in dry AMD [3]. In recent years, research has focused on cell-based treatments for AMD, particularly on differentiating human embryonic stem cells (hESCs) into RPE (termed hESC-RPE) and replacing damaged RPE with hESC-RPE [4]. These hESC-RPE transplantation efforts primarily aim to restore the subretinal physiologic interactions between the RPE and photoreceptors [5, 6].

The two methods primarily used for the subretinal transplantation of hESC-RPE are to inject an hESC-RPE cellular suspension or implant an hESC-RPE monolayer grown on a substrate. However, RPE cells form a polarized monolayer in vivo, between the underlying Bruch's membrane and overlying photoreceptors, and it is questionable whether a cellular suspension can produce the polarization required to restore vision [5]. Therefore, an implant termed CPCB-RPE1, which utilizes an hESC-RPE monolayer cultured on a mesh-supported submicron parylene-C membrane (MSPM; mimicking the Bruch's membrane), has been developed under the auspices of the California Project to Cure Blindness (CPCB) [7, 8]. This implant has been designed to treat patients with dry AMD (dAMD) and severe vision loss by being surgically placed into the subretinal space, replacing the dystrophic RPE and providing physiological support for the overlying photoreceptors.

The present study in the Yucatán minipig was conducted to assess (1) the feasibility of subretinal delivery of CPCB-RPE1, (2) its 1-month safety and tolerability under local or combined local and systemic immunosuppression, and (3) the analysis of the implanted cells by immunohistochemistry approximately 1 month after surgery. This was the first study using CPCB-RPE1 to be conducted in a larger mammalian species whose eyes are similar to human eyes in size and gross retinal anatomy, allowing similar subretinal transplantation techniques to be assessed before human testing.

Materials and methods

Study device

The study device, termed CPCB-RPE1, consisted of a mesh-supported submicron parylene-C membrane (MSPM) and hESC-RPE. The MSPM was vitronectin-coated, overall creating a biocompatible mesh specifically designed to support the culture and subretinal implantation of an hESC-RPE confluent monolayer [7, 9]. Serving as an artificial Bruch's membrane, the MSPM was 6.25 mm in length and 3.5 mm in width, with 0.4 μm (μm) ultra-thin membrane pore areas covering nearly 50 % of the total surface area (Fig. 1a, left).

Before being seeded onto the MSPM, hESCs were cultured in defined conditions using serum-free medium (X-VIVO 10™, Lonza, Walkersville, MD, USA) and Matrigel, and spontaneously differentiated to hESC-RPE through the removal of soluble growth factors. After approximately 100 days, unpigmented cells were manually removed and remaining enriched hESC-RPE cells were passaged using TrypLE™ (Life Technologies, Inc, Bethesda, MD). Second-passage hESC-RPE cells were cryopreserved as an intermediate cell bank. These cultures have been extensively characterized and are 99 % positive for RPE markers [10].

Passage three cells were thawed and then seeded onto MSPM at a density of 10^5 cells/cm^2 and grown to confluence for approximately 4 weeks, achieving a final density of 10^5 cells/MSPM (Fig. 1a, right). Before implantation, implants were checked for confluence, pigmentation, and cobblestone-like morphology of their hESC-RPE monolayers (Fig. 1b). MSPMs that did not meet the quality control criteria were discarded. This process generated a polarized hESC-RPE monolayer with characteristics similar to human fetal RPE which would promote survival of the monolayer in vivo [8, 11].

Animals

Normal-sighted, purpose-bred female Yucatán minipigs (S&S Farms Inc., USA) were used in this study. Animals were housed and fed in facilities approved by the Association for Assessment and Accreditation of Laboratory Animal Care (AAALAC). All study procedures were performed in accordance with the Institutional Animal Care and Use Committee (IACUC) of the University of Southern California (USC).

Animals underwent a baseline and postoperative physical examination (USC Department of Animal Services Veterinarian) and a blinded baseline and postoperative ocular examination by an independent veterinary ophthalmologist. If the veterinarian was unavailable, fundus photographs of the eyes were taken before and after surgical procedures. Animals were anesthetized using weight-based dosing of intramuscular Telazol® (100 mg/ml; Zoetis Inc., Kalamazoo, MI, USA) for baseline examinations and placement of a vascular access port (VAP).

Animals were euthanized by trained staff of the USC Department of Animal Services using a lethal overdose of Euthasol® (Virbac Corp., Fort Worth, TX, USA). Euthanasia was confirmed by clinical assessment of respiration and cardiac function as well as pulse oximetry.

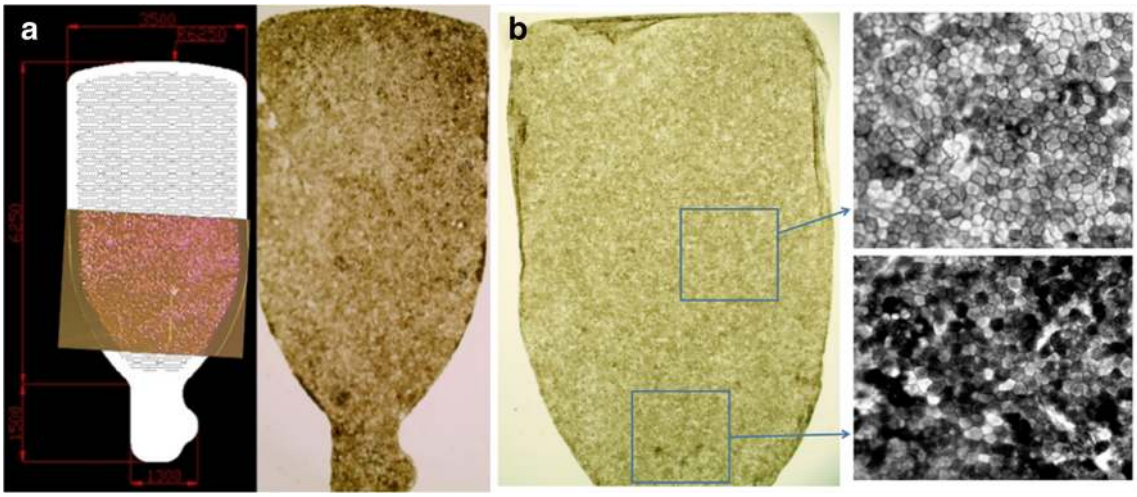

Fig. 1 The CPCB-RPE1 implant. **a** Schematic representation of CPCB-RPE1, with a handle for grasping (small lower portion) and mesh-supported submicron parylene membrane (MSPM; approximately the size of the macular region) serving as a substrate for the hESC-RPE monolayer (shown in the superimposed *inset*) (*left*); uniform pigmented hESC-RPE monolayer at postoperative day 30 (*right*). **b** Confluent hESC-RPE on an MSPM (*left*) and enlarged areas of the monolayer (*right*) demonstrating the cobblestone-like morphology of the hESC-RPE cells

Study design

This was a prospective, partially blinded study in 14 two-month-old, normal-sighted, female Yucatán minipigs, weighing 24–35 kg, to assess the feasibility of subretinal implantation of CPCB-RPE1 and implant safety and tolerability over a 1-month observation period following the surgery. Surgeons were blinded to the randomization codes and post-operative and post-mortem assessments were performed in a blinded manner. The study was conducted at the Department of Ophthalmology, Keck School of Medicine, University of Southern California, Los Angeles, CA, USA from 01-July-2013 to 24-December-2014.

The 14 animals were randomized to one of three study groups. Group 1 consisted of eight animals that underwent surgical implantation of CPCB-RPE1 in the subretinal space and were maintained on both systemic (tacrolimus) and local (Ozurdex™ dexamethasone intravitreal implant; Allergan Inc., Irvine, CA) immunosuppression. Systemic immunosuppression was administered via a VAP surgically placed in the right external jugular vein. Group 2 consisted of three animals that underwent CPCB-RPE1 implantation and local immunosuppression (Ozurdex™) alone. Group 3 consisted of three animals that underwent sham surgery consisting of subretinal bleb creation instead of CPCB-RPE1 implantation and received no immunosuppressant (two animals) or local immunosuppression (one animal). All animals were maintained for ≥30 days unless a change in health status, such as systemic sepsis, warranted euthanasia earlier. All animals were maintained in the group to which they were originally assigned, even if systemic immunosuppression was interrupted or terminated early due to limitations in vascular access or systemic illness.

Optical imaging

Baseline imaging included optical coherence tomography (OCT; Heidelberg Spectralis™, Heidelberg Engineering, Heidelberg, Germany), fluorescein angiograms, and fundus photographs (RetCam™, Clarity Medical Systems Inc., Pleasanton, CA, USA) to document retinal state if an independent clinical examiner was not available. Imaging procedures were similarly repeated at euthanasia for comparative analysis with baseline images unless retinal viewing was obstructed (e.g., due to cataract). Postoperative follow-up imaging was performed unless posterior pole viewing was obscured by corneal, lenticular, or vitreous opacity.

Surgical procedures and postoperative care

Before surgery, anesthesia was induced with intramuscular Telazol® (100 mg/ml; Zoetis Inc., Kalamazoo, MI, USA) and maintained with sevoflurane gas under veterinary supervision. The operative site was prepped and draped with a sterile field after scrubbing with 10 % povidone iodine. Standard vitreoretinal surgical methods and equipment (Stellaris™ PC posterior vitrectomy system, Bausch & Lomb, Rochester, NY, USA) were employed to deliver CPCB-RPE1 to the left eyes of Yucatán minipigs, using the same surgical delivery tool that would be employed in human surgeries. Fine forceps and Wescott scissors were then used to perform a 360° peritomy. A 20-gauge sclerotomy was then made using a micro-vitreoretinal blade at the preplaced suture site and a 20-gauge infusion line placed and secured there. Two additional sclerotomy sites were similarly made at the surgeon's discretion to facilitate ideal retinal access for placement of CPCB-RPE1. Photon light fibers were placed to

facilitate ideal illumination of the intraocular environment. A Zeiss operating microscope (Zeiss Opmi Visu 200/S8, Carl Zeiss Meditec Inc., Dublin, CA, USA) with a binocular indirect ophthalmomicroscope (BIOM; OCULUS Surgical Inc., Port St. Lucie, FL, USA) was used to visualize the intraocular environment. A dissecting microscope and sterile technique were used for preparation of CPCB-RPE1 for intraocular injection as described below.

Intraocular injection of Triesence® (Alcon Laboratories Inc., Fort Worth, TX, USA) was used to help with visualization of the vitreous and vitrectomy (i.e., removal of the vitreous humor) in most cases. At the surgeon's discretion, an area of the retina was selected for the site of retinotomy. Then, a 41-gauge a soft tip cannula mounted on a silicone oil injector was used to access the subretinal space and create a subretinal bleb using an infusion of balanced salt solution (BSS). Before the retinotomy, this site was lasered or diathermized lightly to minimize potential bleeding. During the retinotomy the intraocular pressure was elevated to 60 mmHg to prevent any bleeding. Next, one of the sclerotomies was enlarged by 1–2 mm using a microvitreoretinal blade to allow insertion of a custom-made delivery tool. Animals that were in the sham group only underwent this portion of the procedure and none of the subsequent steps except for closure of the wounds.

During the vitrectomy, and at the surgeon's discretion, the CPCB-RPE1 was retrieved from a standard cell culture incubator (in the same building as the surgical suite) by an assistant and then removed from the culture medium with sterile forceps using the implant's accessory tab (which was designed for this purpose). The surgeon then sterilely cut off the accessory tab under a dissecting microscope and loaded the implant into the custom-made delivery tool (Synergetics Inc., O'Fallon, MO, USA). The tool's tip remained submerged in BSS for 8 to 13 min, at which point the surgeon implanted the CPCB-RPE1 in the subretinal space. To deliver CPCB-RPE1, the pre-loaded delivery tool described above was inserted into the eye and the tip carefully placed into the subretinal space through the above-described retinotomy. Once the tool's tip was properly localized, CPCB-RPE1 was delivered into the subretinal space and the delivery tool removed. Nearly simultaneously, the eye was instilled with perfluorocarbon liquid to flatten the bleb and prevent the implant from extruding through the retinotomy. The perfluorocarbon was removed with a soft tip cannula and replaced with air. The retina was inspected for bleeding or signs of retinal detachment and attempts were made to treat any such problems. Finally, a silicone oil injector was used to replace the air with 1000 or 5000 centistoke silicone oil. The infusion line was removed and the sclerotomies and overlying conjunctiva closed using 6–0 vicryl suture.

Postoperative examinations were performed on postoperative day 1, week 1 and then weekly thereafter unless any complications or problems were noted. All animals were monitored by veterinary staff for normal behaviors, including feeding, drinking, urination, and stools. Animals received buprenorphine for postoperative pain management as well as topical Maxitrol® ointment (Alcon Laboratories Inc., Fort Worth, TX, USA) for infection and inflammation prophylaxis during the first postoperative week, as needed.

Histology and immunohistochemistry

After sacrifice, surgically treated eyes were enucleated using standard, globe-preserving surgical techniques and prepared for histologic examination of the implantation site. All harvested eyes were fixed in Davidson's solution, preserved in formalin, and then cut in half to remove the posterior half but retain the quadrant containing the implant or subretinal bleb. The retained region was embedded in paraffin and serially sectioned into 5-μm-thick slices using a microtome.

Hematoxylin-eosin (HE) staining was performed on every 10th slide of all serially sectioned eye tissues to histologically visualize cells on the implant. HE-stained slides were scanned using the Aperio Scanscope CS microscope hardware and software (Aperio Technologies Inc., Vista, CA, USA). After scanning, images of each slide were taken at 2×, 4×, and 10× magnification to archive and analyze the images. To check for the safety of the surgery, the placement of the CPCB-RPE1 was evaluated in a masked manner and determined as the percentage of the implant in the subretinal space.

Immunohistochemistry staining for TRA-1-85 and RPE65 (a human marker and an RPE marker, respectively) was performed to identify hESC-RPE cells. One slide from each sample was stained. Slides were deparaffinized and rehydrated before staining. Slides were incubated with the following primary antibodies overnight at 4 °C: monoclonal mouse anti-TRA-1-85 (R&D Systems Inc., Minneapolis, MN, USA; MAB3195; 1:100) and polyclonal rabbit anti-RPE65 (Abcam plc, Cambridge, UK; Ab105366; 1:500). Slides were incubated with the appropriate rhodamine or FITC-conjugated secondary antibodies (Jackson ImmunoResearch Laboratories Inc., West Grove, PA, USA; 117098 and 113127; both 1:100) for 1 h at room temperature and then mounted with fluorescent-enhance mounting medium containing 4',6-diamidino-2-phenylindole (DAPI; Vector Laboratory Inc., Burlingame, CA, USA). Images were acquired using an Ultraviewer ERS dual spinning disk confocal microscope (PerkinElmer, Waltham, MA, USA) equipped with a C-Apochromat 10× high dry lens, a C-Apochromat 40× water immersion lens NA 1.2 and an electron multiplier CCD cooled digital camera. All slides were scanned under the same conditions for magnification, brightness, and gain. Images were captured and processed using Volocity® 3D Image Analysis Software (PerkinElmer). Scoring of immunostained slides was standardized. TRA-1-85/RPE65 scoring was set at four levels: negative (−), weakly positive (+), moderately

positive (++), and strongly positive (+++). The scoring criteria for TRA-1-85/RPE65 combined previous staining experience and comparison of several stained slides from this study.

Data collection and analysis

The data of primary interest in this study were nonnumerical. No statistical analysis or tests were conducted.

Results

Clinical findings

Baseline examination of the eyes in all minipigs revealed no major abnormalities, except for occasional microscopic hemorrhage in the retinal periphery in one animal. Upon baseline examination, intraocular pressures were also within normal limits (10–20 mmHg). Postoperatively, minipigs were maintained for a median (range) observation period of 31 (13–43) days. Table 1 summarizes the animals' clinical characteristics.

All animals that received CPCB-RPE1 underwent the subretinal implantation successfully; expected postoperative observations (mild bleeding in the vitreous/oil space in two animals; elevated intraocular pressure up to 24 mmHg in one animal) within 2 days after surgery were transient and did not result in rejection of the implant. Comprehensive postoperative clinical examination of the operated eye demonstrated expected, but clinically insignificant, postoperative changes associated with vitrectomy, e.g., mild conjunctival congestion, conjunctival hyposphagma, mild cataract, and subconjunctival hemorrhage in all animals. These changes generally resolved within 1–2 weeks of surgery. One animal that received CPCB-RPE1 developed a focal peripheral retinal detachment during surgery that was successfully treated intraoperatively by means of fluid–air exchange, drainage of subretinal fluid, and peripheral laser coagulation. There were no other sequelae or consequences for the CPCB-RPE1, which was implanted at the central retina. Intraocular pressures did not change markedly in the postoperative period and remained below 20 mmHg. All vitrectomy wounds healed normally and without complications in all animals.

Implant placement and retinal findings

Postoperative clinical examination of the posterior segment of the retina in vivo demonstrated subretinal location of all CPCB-RPE1 in all animals except one, in which <50 % of the implant was located subretinally, the remainder of the implant, especially its handle, being located intraretinally. Fundus imaging demonstrated good subretinal placement without any gross defects, bends or folds in 6/8 (75 %) minipigs in group 1. No breaks were observed in the implanted CPCB-RPE1 membranes. Mild bends in the handle

Table 1 Clinical course and immunohistochemistry results for CPCB-RPE1 implantation

Pig ID	Implant duration	Treatment group	Immunosuppression[a]	Implant position	Histology available[b]	TRA-1–85	RPE65	Comments
Group 1: CPCB-RPE1 implantation with combined systemic (tacrolimus, Tac) and local (Ozurdex™, Ozx) immunosuppression								
A	32 days	CPCB-RPE1	Tac + Osx (100 %)	Subretinal	Yes	+++	++	—
B	40 days	CPCB-RPE1	Tac + Osx (80 %)	Subretinal	Yes	+++	+++	Animal removed VAP[c] multiple times
C	42 days	CPCB-RPE1	Tac + Osx (100 %)	Subretinal	Yes	+	++	—
I	13 days	CPCB-RPE1	Tac + Osx (100 %)	Subretinal	No	N/A	N/A	Euthanized early due to sepsis
L	18 days	CPCB-RPE1	Tac + Osx (100 %)	Subretinal	Yes	++	++	Euthanized early due to sepsis
M	30 days	CPCB-RPE1	Tac + Osx (100 %)	Subretinal	Yes	++	+	—
N	22 days	CPCB-RPE1	Tac + Osx (41 %)	N/A[d]	Yes	+	+	Euthanized early due to sepsis
O	34 days	CPCB-RPE1	Tac + Osx (85 %)	Subretinal	Yes	+++	++	Animal removed VAP[c] at least once
Group 2: CPCB-RPE1 implantation with local (Ozurdex™, Osx) immunosuppression								
D	35 days	CPCB-RPE1	Osx	Subretinal	Yes	+++	++	—
E	43 days	CPCB-RPE1	Osx	Subretinal	Yes	N/A	N/A	—
J	33 days	CPCB-RPE1	Osx	Subretinal	Yes	+	+	—
Group 3: Sham surgery with bleb formation and combined systemic (tacrolimus, Tax) and local (Ozurdex™, Osx) immunosuppression or no immunosuppression								
H	14 days	Sham	Tac + Osx (0 %)	Sham	No[b]	N/A	N/A	Euthanized early due to sepsis
R	28 days	Sham	None	Sham	Yes	N/A	N/A	—
S	26 days	Sham	None	Sham	Yes	N/A	N/A	—

[a] Percentages represent the percentage of days on which animals received all scheduled doses of tacrolimus in the postoperative period until euthanasia; 0 % indicates that the animal only received preoperative doses of tacrolimus and could not tolerate the medication beyond a few days

[b] Histology was not available for some specimens because the implant could not be located in the enucleated eye for processing

[c] *VAP* Vascular access port

[d] *N/A* The position of the CPCB-RPE1 implant was not confirmed by imaging at the time of euthanasia due to poor view secondary to cataracts or other media opacity

region of the implant were noted in two cases but this did not affect the subretinal placement as demonstrated by histology. Figures 2 and 3 show representative images of the subretinal placement from two different group 1 animals on the day of sacrifice. Longitudinal and transverse OCT studies demonstrated that the handle and body of the implant were in a subretinal location in all implanted animals. In all animals, at the time of sacrifice there was no evidence of adverse reactions or clinical complications such as intraretinal edema or subretinal fluid, and fluorescein angiography demonstrated minimal staining of the membrane and overlying retina, indicating an absence of adverse neovascularization.

As expected, in all cases where the handle of the CPCB-RPE1 implant was adjacent to or underneath the retinotomy site, there was thinning of the overlying retina on OCT images, as shown in Fig. 2. This was consistent with the appearance of chorioretinal scarring on the retina in this area, which was due to the thermal damage caused by laser and diathermy treatments during surgery. In addition, retinal thinning was also present in control animals that had undergone laser or diathermy but no CPCB-RPE1 implantation, confirming that the overlying retinal thinning was due not to the implant but to the laser treatment at the retinotomy site, which is expected. In no case was there a retinal detachment, hemorrhage or protrusion of the handle through the retina. In cases where the handle of the CPCB-RPE1 implant was positioned further away from the retinotomy site (7/11 pigs), there was no thinning of the overlying retina, suggesting that the handle by itself did not have an adverse effect on the overlying retina (Fig. 3).

Vascular access port-related observations

All eight group 1 animals and one group 3 control in our 1-month study were assigned to receive VAPs for systemic immunosuppression (Table 1). Of these nine animals, four (44 %; three from group 1 and the systemically immunosuppressed control) were euthanized early due to sepsis between 1 and 3 weeks after VAP placement, and two others (22 %) from group 1 dislodged their VAPs at least once, resulting in an incomplete course of immunosuppression. Therefore, only 3/9 (33 %) animals undergoing systemic immunosuppression (pigs A, C, and M) completed the 1-month study as planned. Two of the four animals that were euthanized early showed signs of endogenous endophthalmitis and infectious chorioretinitis secondary to ocular seeding of bacteria. One of these animals had a serous retinal detachment but no

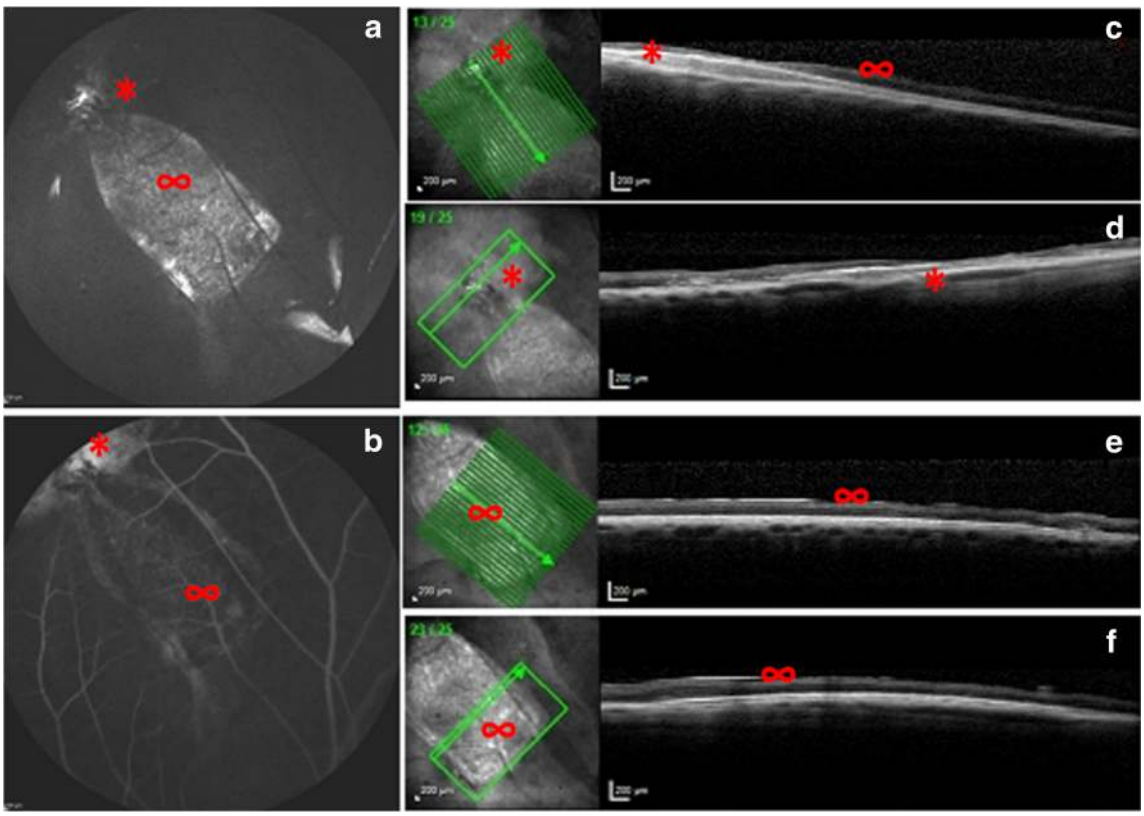

Fig. 2 Imaging and histology results from pig A (group 1). **a** Infrared image of the subretinal implant. **b** Late phase fluorescein angiogram of the implant illustrating minimal hyperfluorescence changes. **c**, **d** Optical coherence tomographs (OCTs) illustrating longitudinal and horizontal cross sections of the implant handle (*). There is evidence of focal laser and retinal thinning near the area of the retinotomy. **e**, **f** OCTs illustrating longitudinal and horizontal cross sections of the implant body (∞)

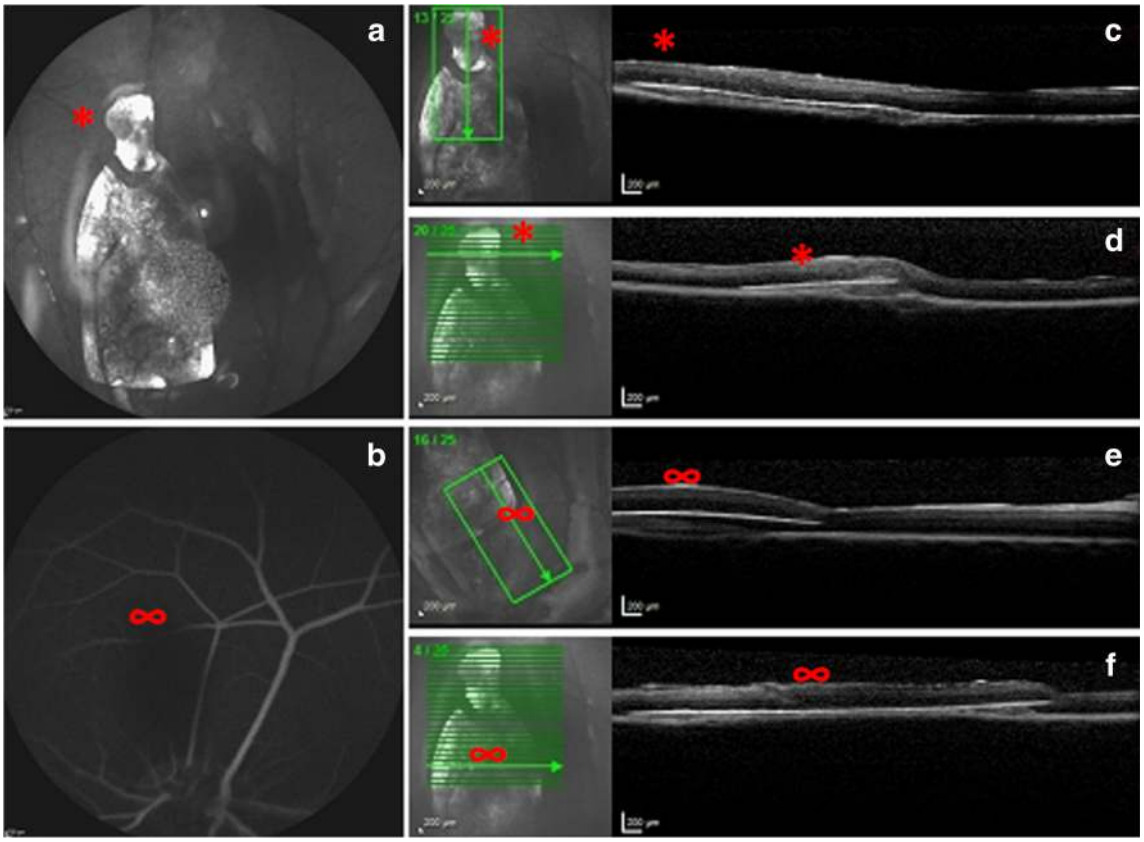

Fig. 3 Imaging and histology results from pig C (group 1). **a** Infrared image of the subretinal implant. **b** Late-phase fluorescein angiogram of the implant region illustrating minimal hyperfluorescence changes. **c**, **d** Optical coherence tomographs (OCTs) illustrating longitudinal and horizontal cross sections of the implant handle (*). **e**, **f** OCTs illustrating longitudinal and horizontal cross sections of the implant body (∞)

rhegmatogenous retinal detachment. None of these findings were associated with the surgical procedure or the implant itself. The study data are summarized in Table 1.

Histology and immunohistochemistry

Histological analysis was available on 10/11 animals receiving CPCB-RPE1 (groups 1 and 2) and 2/3 sham-operated (group 3) animals. As shown in Table 2, nine of the ten eyes (90 %) with the implant exhibited satisfactory implant placement; seven of these satisfactorily placed implants (77.8 %) had 100 % of the implant located in the subretinal space. Only 1/10 (10 %) of the implanted eyes (from group 1) had <50 % of the implant located subretinally (with the majority of the implant located intraretinally). As regards sham surgery, which involved the creation and immediate intraoperative draining of a subretinal bleb, histology revealed some scarring of the outer retina but no defect of the adjacent retina.

In the seven animals that had CPCB-RPE1 positioned entirely in the subretinal space, the retinal structure remained largely intact with only minimal changes, such as focal disruption and slight inner nuclear layer (INL) thinning. Normal INL structure and thickness was observed in 6/10 (60 %) of eyes, focal disruption due to the implant but retention of normal INL thickness was observed in 1/10 (10 %) of eyes, and focal disruption accompanied by focally thinned INL overlying the implant was observed in 2/10 (20 %) of eyes. Most samples (8/10, 80 %) showed some thinning of the outer nuclear layer (ONL) overlying the CPCB-RPE1. Although the neural retina and RPE were artifactually separated as a result of tissue processing, the properly oriented inner and outer segments of photoreceptors and a lack of a debris zone suggested that interdigitation between host photoreceptor outer segments and apical sides of the implanted human RPE in the CPCB-RPE1 was present in most eyes (9/10). Only one eye, which had extensive intraretinal instead of the anatomically correct subretinal placement, showed significant damage to the retinal structure, including atrophy and fibrosis. All examined implanted eyes (10/10; 100 %) displayed normal host RPE and choroid morphology.

No local inflammatory response was observed in any of the eyes. In 3/10 (30 %) of eyes, focal, mild fibrosis was observed; two of these eyes had focal fibrosis at the basal side of the CPCB-RPE1, and the remaining one eye had a small focal area of fibrosis in the choroid. None of the eyes had peri-implant fibrosis.

Table 2 Histological analysis of retinal structure and host response in minipigs receiving CPCB-RPE1 implants

Pig ID	Group	Percentage of implant in subretinal space	Host retinal structure				Host tissue response	
			Host INL	Host ONL	Host RPE	Host choroid	Chronic inflammation	Fibrosis
A	1	100	Normal	Thinned (2 layers)	Normal	Normal	–	–
B	1	100	Normal	Thinned (2 layers)	Normal	Normal	–	+ Focally in choroid
C	1	85	Focally disrupted by implant, otherwise normal	Normal thickness	Normal	Normal	–	+ At the basal side of implant
L	1	100	Focally thinned	Focally thinned. Partial rosette.	Normal	Normal	–	–
M	1	100	Normal	Thinned (3–6 layers)	Normal	Normal	–	–
N	1	Intraretinal	Disrupted	Disrupted	Normal	Normal	–	–
O	1	100	Normal	Normal thickness	Normal	Normal	–	–
D	2	100	Normal	Thinned (4–6 layers)	Normal	Normal	–	+ Focally at the basal side of implant
E	2	100	Normal	N/A	N/A	N/A	N/A	N/A
J	2	95	Focally disrupted and thinned	Thinned (1–5 layers). Partial rosette	Normal	Normal	–	–

INL inner nuclear layer, *ONL* outer nuclear layer, *RPE* retinal pigment epithelium, *N/A* not available

Histological analysis of hESC-RPE on CPCB-RPE1 after implantation revealed that all eyes (10/10; 100 %) had a single layer of pigmented and cobblestone-shaped cells regularly aligned on the implant, as visualized using hematoxylin-eosin (HE) staining (Fig. 4). Immunohistochemical staining demonstrated that the CPCB-RPE1 cells were positive for the human and RPE markers TRA-1-85 and RPE65, indicating that the hESC-RPE cells in those samples had survived 1 month of implantation (Fig. 4 and Table 1). The host RPE cells were strongly positive for RPE65.

Histological analysis of the region surrounding the implant handle revealed expected focal cell loss, when it was adjacent to the retinotomy site. The CPCB-RPE1 implant handle was designed and manufactured for manipulation of the CPCB-RPE1 during the process of loading it into the surgical injector tool, so possible focal cell damage and focal denting, as well as bending of the handle itself, were anticipated. The handle of the CPCB-RPE1 implant was identified histologically (Fig. 5) based on width (1–1.5 mm for the handle and 3.5 mm for the body) and by the absence of ultrathin areas, which are only found on the body of the MSPM. In the five pig eyes with definitively identifiable handles, one handle (1/5; 20 %) demonstrated focal denting and bending (see pig B in Fig. 5), while all five (100 %) handles showed focal cell loss and partial intraretinal implantation with associated pathology. Intraretinal location was most common at the distal end of the handle, i.e., the area furthest from the body. Sections of the handle taken closer to the implant's body were flat and entirely positioned within the subretinal space. To avoid implant intraretinal location, complete subretinal placement should be achieved in future applications.

Discussion

The present study in 14 Yucatán minipigs is the first investigation of surgical subretinal delivery of the CPCB-RPE1 implant, an hESC-derived RPE monolayer on an MSPS carrier, in a mammalian species whose eye is similar to the human eye in size and gross retinal anatomy, allowing similar subretinal transplantation techniques to be assessed before human testing. The advantages of the surgically foldable MSPS carrier include customized macular shape in diameter and thickness [8], ultrathin parts with diffusion [7], and excellent RPE adherence [10, 11] and survival [12], whereas its non-degradability and unknown long-term effects can be seen as disadvantages. The study criteria for successful implantation were appropriate placement of the implant in the subretinal space, as assessed by OCT and post-mortem histology. The study demonstrated that the CPCB-RPE1 can be reliably implanted into the subretinal space of the swine eye using surgical techniques similar to those that would be used in humans. Thorough in vivo examinations demonstrated safe placement

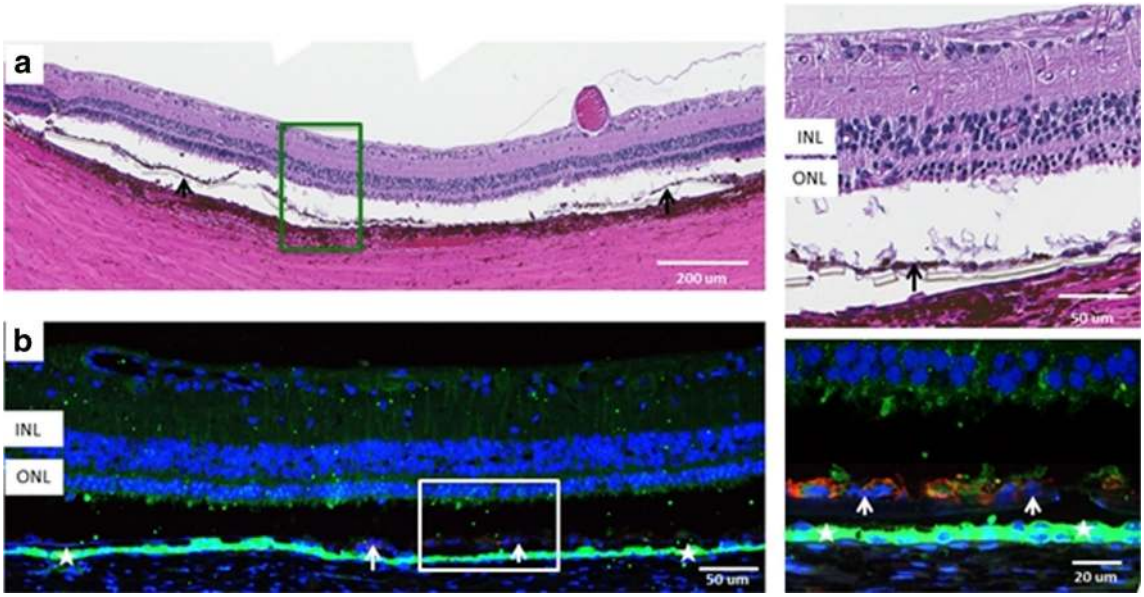

Fig. 4 Representative histological images of pig retina 1 month after receiving CPCB-RPE1 implant and immunosuppression with intravenous tacrolimus and an intravitreal dexamethasone implant. **a** Histology of hematoxylin-eosin stained eye section. **b** Immunohistochemical staining of TRA-1-85 (red), RPE65 (green), and nuclei (blue; utilizing DAPI). Areas indicated by rectangles in **a** and **b** are magnified on the right. Implanted hESC-RPE overlying the mesh-supported submicron parylene membrane (MSPM) with alternating ultrathin and thick areas (*arrows*, *black* and *white*) and host RPE (*white stars*) is indicated. *INL* inner nuclear membrane; *ONL* outer nuclear membrane

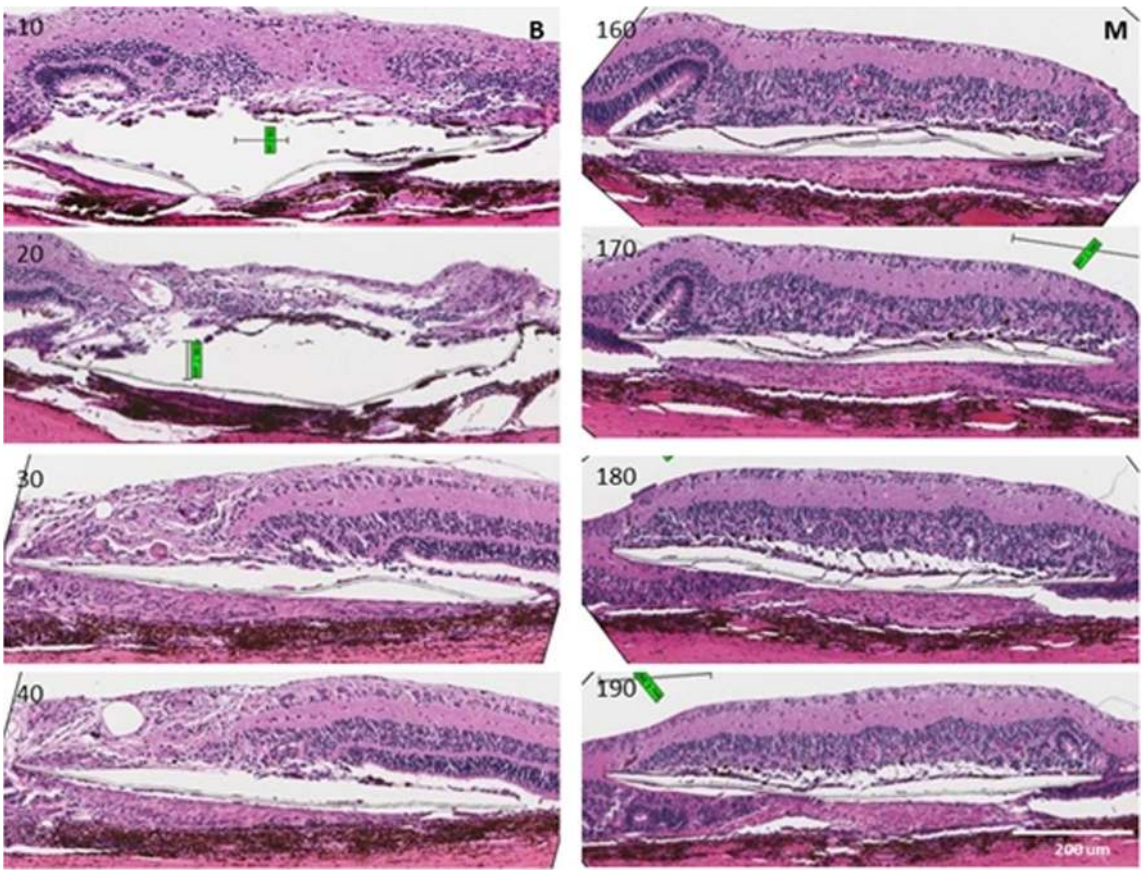

Fig. 5 Histological images of hematoxylin-eosin stained pig retinas from two representative implanted samples (pig B, *left*, and pig M, *right*), both from group 1 and showing the handle of the CPCB-RPE1 implant. *Slide numbers* are indicated in the left upper corners. Areas of retinal atrophy and disorganization in the region of the handle correspond with areas of laser and/or diathermy during surgery

of the implant without severe clinical complications, e.g., postoperative endophthalmitis, intraocular hypotension or hypertension, or retinal detachment. Moreover, while surgical implantation of CPCB-RPE1 into a normal eye was expected to result in some damage to the overlying retina, retinal basic structure remained intact with only minimal changes when the implant was placed entirely in the subretinal space. No breakage of the CPCB-RPE1 was observed. Histology demonstrated that the RPE cells in the CPCB-RPE1 survived as an intact monolayer after implantation. There was also no evidence of a local inflammatory response or peri-implant fibrosis in any of the eyes. In line with an earlier study we conducted in rats [12], no formation of teratoma or ectopic tissue was observed in the minipig eye. Immunohistochemistry for TRA-1-85 and RPE65 was positive in all of the CPCB-RPE1 implants, indicating that the hESC-RPE cells survived in those samples after 1 month of implantation. Of note, RPE65 was also labeled in the outer segments of a subset of host photoreceptors, which is consistent with a report that RPE65 is found in outer segments of a subset of cones (green/red) [13]. However, the necessity or benefit of systemic tacrolimus or local dexamethasone immunosuppression for this procedure remains unclear due to the variability of maintaining swine on systemic immunosuppression. The safety and tolerability issues encountered in this study were related to VAP dislodgement, VAP site infection, and the resulting sepsis in the systemically immunosuppressed animals rather than to the implant or the surgical procedure as such. In several cases there were interruptions in the immunosuppression regimen from either unanticipated removal of VAPs by the animals themselves or surgical removal of the ports due to surgical site infections. Therefore, the role of immunosuppression in the survival of this implant is unclear. However, the fact that there were interruptions of immunosuppression and the lack of any focal inflammatory response around the CPCB-RPE1 implant suggest that systemic immunosuppression may not be necessary for survival of CPCB-RPE1 in the subretinal space in minipigs.

Cell-based subretinal implantation using carrier substrates is surgically feasible. RPE transplantation in the pig is a relatively young field, and surgical implications of such implantations have not been fully explored [14–21]. Human autologous RPE transplantation studies, primarily in patients with exudative AMD, have shown that intraoperative complications are infrequent [22–24]. No such complications were observed in our study. Early and late postoperative complications in human subjects, however, have included intraocular hemorrhage, serous macular detachment, epiretinal membrane formation, the development of proliferative vitreoretinopathy, or the induction of choroidal neovascularization in a patient who previously had dAMD [23, 25].

In the present study, our surgical technique did not cause any retinal or choroidal bleeding, a potential complication reported to occur in eight of 11 pigs after autologous RPE-choroid graft transplantation [20]. We created a subretinal bleb before the insertion of our transplant. The effects of bleb creation have been investigated, mostly in rabbits [26]. Our study primarily aimed to investigate the surgical safety of hESC-RPE transplantation with regard to, e.g., retinal detachment or proliferative vitreo-retinopathy. However, it may be considered a potential limitation of our study that we did not prospectively examine retinal response using multifocal electroretinography (mfERG). Christiansen et al. elaborated this sensitive technique and were able to provide reliable data on the electrophysiologic dependencies of different subretinal materials [18, 27]. Although we had no robust mfERG setup in place and would endorse including mfERG in future studies, we feel confident regarding the biocompatibility of the material with and without cells due to our experience with the optokinetic nystagmus and superior colliculus recordings in the RCS rat (data submitted to FDA with an Investigational New Drug submission; this aspect is also discussed in a recent review article by our group [28]). We observed normal INL structure and thickness in most (60 %) eyes, focal implant-related disruption in some (30 %) cases and some ONL thinning in the implantation area in the majority (80 %) of eyes. Despite some tissue processing-related artifacts, histology suggested that interdigitation between host photoreceptor outer segments and apical sides of the implanted human RPE was present in almost all (90 %) eyes.

In humans, it is widely accepted that the RPE is anchorage dependent; RPE cells must attach to an adequate Bruch's membrane-like substrate to avoid cell death [29, 30]. Del Priore and coworkers observed allogeneic RPE graft survival in non-immunosuppressed pigs for up to 3 months without surgical RPE debridement, but this was associated with marked shortening of the outer segments and a multilayer of heavily pigmented RPE [14]. Others performed a surgical RPE debridement before RPE transplantation and observed RPE proliferation and decreased photoreceptor loss [16, 31]. In our setup, which was without a debridement because we primarily investigated the surgical safety of hESC-RPE transplantation, we did not encounter any T-cell mediated immunohistologic reaction from the host RPE or any fluid accumulation around the transplant, such as macular edema. In AMD the decline in hydraulic conductance of Bruch's membrane is very important;

it may lead to RPE detachment and lipid accumulation [32, 33]. One future experimental setup for our technique would be to incorporate RPE debridement to address various pitfalls, e.g., retinal bleb creation in atrophic regions, in human subretinal AMD surgery. Any subretinal transplantation, with or without synthetic implants, must have adequate hydraulic conductance to prevent pooling of fluid at the RPE substrate interface [34]. In our non-aged pigs, fluorescein angiography demonstrated no fluid pooling, neovascularization, or insufficient perfusion of the retina or choroid associated with implantation. Patent physiologic vascularization supports our previous MSPM biocompatibility testing and the impression from the RCS rat surgeries, where none of these issues linked to decreased conductance were observed [7, 8].

Unlike Warfvinge et al. [21], who observed large choroidal infiltrates 2–5 weeks after subretinal transplantation of murine retinal progenitor cells derived from non-immunosuppressed mice, we found that all studied eyes with immunosuppression presented a normal choroid. Del Priore observed no significant inflammatory response after non-immunosuppressed allogeneic porcine RPE sheet transplantation [14]. In pilot studies, in which we performed larger retinotomies using larger transplantation tools and had up to 14 weeks' follow-up with no immunosuppression, we encountered severe choroidal inflammatory reactions after surgery [35]. Our decision to employ immunosuppression is also in accordance with the only human hESC-RPE trial, which used low-dose tacrolimus and mycophenolate mofetil to prevent RPE rejection, but we primarily advocate minimalistic surgery, as applied here, so as not to unduly compromise the subretinal space [4]. Using combined systemic tacrolimus and local dexamethasone or local dexamethasone alone for immunosuppression in the present study, we obtained greatly improved in vivo imaging and ex vivo histological results compared to no immunosuppression, even if systemic immunosuppression was frequently incomplete due to VAP dislodgement. Our immunostaining demonstrated an absence of inflammatory cells, indicating an absence of host reaction to the CPCB-RPE1.

Several strengths and limitations warrant discussion. Animals were randomized to CPCB-RPE1 implantation or sham surgery and surgeons were blinded to randomization codes and to whether or not animals were to receive systemic tacrolimus. However, the study was of a limited size and its design did not require balanced groups. In addition, VAP dislodgement resulted in incomplete systemic immunosuppression, thus obscuring the role of immunosuppression for hESC-RPE survival. Moreover, we cannot preclude that the sepsis warranting early euthanasia in the 3/8 animals receiving both the CPCB-RPE1 and combined systemic and local immunosuppression was related to the immunosuppressants. To clarify the importance of immunosuppression the study design would need to incorporate appropriate controls and, most likely, a follow-up period of more than 30 days. Another limitation was a lack of fundus autofluorescence (FAF) imaging, which would have yielded an in vivo understanding of the transplanted hESC-RPE. The study was also limited by the time frame; testing over a longer follow-up period would have been more informative. We experimented with using multifocal electroretinography, different from the type used by Kyhn et al. in a pilot surgery [18], but encountered too much noise to obtain reliable in vivo data. Overall, we believe that a sustained and successful RPE transplantation mandates the safe transplantation of a polarized monolayer to physiologically achieve or maintain visual acuity and avoid cell death over time. Finally, there are certain differences between the swine and human eye that limit which surgical methods can successfully be used in this animal compared to in humans [36]. Nonetheless, the minipig eye can be considered sufficiently similar to the human eye to serve as an in vivo model for retinal surgery studies.

Conclusions

Our study shows it is feasible to successfully and reliably deliver the CPCB-RPE1 into the subretinal space of the Yucatán minipig eye using a custom-made surgical delivery tool along with tools and methods commonly used in human vitreoretinal surgery. In the vast majority of cases (91 %), clinical examination, imaging and histological analysis showed that the CPCB-RPE1 implant remained in the subretinal space for the duration of implantation, even if 10–20 % of the implant had intraretinal localization histologically. Furthermore, overall retinal preservation was demonstrated via in vivo imaging and histology of the ONL and photoreceptor outer segment overlying the implant. Minimal retinal changes observed could be easily attributed to diathermy and laser photocoagulation that was used as a standard part of the surgery. There was no evidence of adverse events, retinal detachment, or focal inflammation associated with the body of the implant. Notably, there was no instance of retinal detachment despite histological evidence of focal denting and bending of the implant handle at the site of manipulation by the custom surgical tool. Moreover, there was no breakage of the CPCB-RPE1 implant in any case. In conclusion, although our study was inconclusive regarding the necessity or benefit of systemic or local immunosuppression, it demonstrated the feasibility and safety of CPCB-RPE1 subretinal implantation in an animal model comparable to the human eye. We are confident that our study provides an encouraging starting point for early human studies.

Acknowledgments This work is supported by the California Institute for Regenerative Medicine DR1-01444, TG2-01161, TG2-01151, CL1-00521 and FA1-00616 grants, NIH Core Grant EY03040, Research to Prevent Blindness, The Arnold and Mabel Beckman Foundation, The Beatrice Apple Revocable Living Trust, The Garland Initiative for Vision, The Foundation Fighting Blindness Wynn-Gund Translational Research Acceleration Program, and the UCSB Institute for Collaborative Biotechnologies through grant W911NF-09-0001 from the U.S. Army Research Office. The content of the information does not necessarily reflect the position or the policy of the Government, and no official endorsement should be inferred. Michael Koss received a research fellowship grant from the German Research Foundation (DFG), Bonn, Germany (DFG Ko4294/1-1). The authors thank Ernesto Baron and his team for excellent technical assistance with the histology. We also thank J. Cito Habicht, PhD, and Teisha R. Rowland, PhD, who provided writing and editing assistance.

Compliance with ethical standards

Funding The California Institute for Regenerative Medicine provided financial support in the form of grant funding (DR1-01444, TG2-01161, TG2-01151, CL1-00521, and FA1-00616). The U.S. National Institutes of Health provided financial support in the form of grant funding (NIH Core Grant EY03040). Research to Prevent Blindness, The Arnold and Mabel Beckman Foundation, The Beatrice Apple Revocable Living Trust, The Garland Initiative for Vision, The Foundation Fighting Blindness Wynn-Gund Translational Research Acceleration Program, and the UCSB Institute for Collaborative Biotechnologies provided financial support through grant W911NF-09-0001 from the U.S. Army Research Office. The content of the information does not necessarily reflect the position or the policy of the U.S. Government, and no official endorsement should be inferred. The German Research Foundation (DFG), Bonn, Germany provided financial support in the form of a research fellowship grant to Michael J. Koss (DFG Ko4294/1-1).

The sponsors had no role in the design or conduct of this research.

Conflict of interest MSH, DRH, and DOC are co-founders of Regenerative Patch Technologies (RPT), LLC. All other authors certify that they have no affiliations with or involvement in any organization or entity with any financial interest (such as honoraria; educational grants; participation in speakers' bureaus; membership, employment, consultancies, stock ownership, or other equity interest; and expert testimony or patent-licensing arrangements), or non-financial interest (such as personal or professional relationships, affiliations, knowledge or beliefs) in the subject matter or materials discussed in this manuscript.

Ethical approval All applicable international, national, and/or institutional guidelines for the care and use of animals were followed. All procedures performed in studies involving animals were in accordance with the ethical standards of the institution or practice at which the studies were conducted.

References

1. Lim LS, Mitchell P, Seddon JM, Holz FG, Wong TY (2012) Age-related macular degeneration. Lancet 379(9827):1728–1738. doi:10.1016/S0140-6736(12)60282-7
2. Peyman GA, Blinder KJ, Paris CL, Alturki W, Nelson NC Jr, Desai U (1991) A technique for retinal pigment epithelium transplantation for age-related macular degeneration secondary to extensive subfoveal scarring. Ophthalmic Surg 22(2):102–108
3. Algvere PV, Berglin L, Gouras P, Sheng Y, Kopp ED (1997) Transplantation of RPE in age-related macular degeneration: observations in disciform lesions and dry RPE atrophy. Graefes Arch Clin Exp Ophthalmol 235(3):149–158
4. Schwartz SD, Hubschman JP, Heilwell G, Franco-Cardenas V, Pan CK, Ostrick RM, Mickunas E, Gay R, Klimanskaya I, Lanza R (2012) Embryonic stem cell trials for macular degeneration: a preliminary report. Lancet 379(9817):713–720. doi:10.1016/S0140-6736(12)60028-2
5. Binder S, Stanzel BV, Krebs I, Glittenberg C (2007) Transplantation of the RPE in AMD. Prog Retin Eye Res 26(5):516–554. doi:10.1016/j.preteyeres.2007.02.002
6. da Cruz L, Chen FK, Ahmado A, Greenwood J, Coffey P (2007) RPE transplantation and its role in retinal disease. Prog Retin Eye Res 26(6):598–635. doi:10.1016/j.preteyeres.2007.07.001
7. Lu B, Zhu D, Hinton D, Humayun MS, Tai YC (2012) Mesh-supported submicron parylene-C membranes for culturing retinal pigment epithelial cells. Biomed Microdevices 14(4):659–667. doi:10.1007/s10544-012-9645-8
8. Hu Y, Liu L, Lu B, Zhu D, Ribeiro R, Diniz B, Thomas PB, Ahuja AK, Hinton DR, Tai YC, Hikita ST, Johnson LV, Clegg DO, Thomas BB, Humayun MS (2012) A novel approach for subretinal implantation of ultrathin substrates containing stem cell-derived retinal pigment epithelium monolayer. Ophthalmic Res 48(4):186–191. doi:10.1159/000338749
9. Rowland TJ, Blaschke AJ, Buchholz DE, Hikita ST, Johnson LV, Clegg DO (2013) Differentiation of human pluripotent stem cells to retinal pigmented epithelium in defined conditions using purified extracellular matrix proteins. J Tissue Eng Regen Med 7(8):642–653. doi:10.1002/term.1458
10. Pennington BO, Clegg DO, Melkoumian ZK, Hikita ST (2015) Defined culture of human embryonic stem cells and xeno-free derivation of retinal pigmented epithelial cells on a novel, synthetic substrate. Stem Cells Transl Med 4(2):165–177. doi:10.5966/sctm.2014-0179
11. Hsiung J, Zhu D, Hinton DR (2015) Polarized human embryonic stem cell-derived retinal pigment epithelial cell monolayers have higher resistance to oxidative stress-induced cell death than nonpolarized cultures. Stem Cells Transl Med 4(1):10–20. doi:10.5966/sctm.2014-0205
12. Diniz B, Thomas P, Thomas B, Ribeiro R, Hu Y, Brant R, Ahuja A, Zhu D, Liu L, Koss M, Maia M, Chader G, Hinton DR, Humayun MS (2013) Subretinal implantation of retinal pigment epithelial cells derived from human embryonic stem cells: improved survival when implanted as a monolayer. Invest Ophthalmol Vis Sci 54(7):5087–5096. doi:10.1167/iovs.12-11239
13. Tang PH, Buhusi MC, Ma JX, Crouch RK (2011) RPE65 is present in human green/red cones and promotes photopigment regeneration in an in vitro cone cell model. J Neurosci 31(50):18618–18626. doi:10.1523/JNEUROSCI.4265-11.2011
14. Del Priore LV, Tezel TH, Kaplan HJ (2004) Survival of allogeneic porcine retinal pigment epithelial sheets after subretinal transplantation. Invest Ophthalmol Vis Sci 45(3):985–992
15. Guduric-Fuchs J, Chen W, Price H, Archer DB, Cogliati T (2011) RPE and neuronal differentiation of allotransplantated porcine ciliary epithelium-derived cells. Mol Vis 17:2580–2595
16. Kiilgaard JF, Prause JU, Prause M, Scherfig E, Nissen MH, la Cour M (2007) Subretinal posterior pole injury induces selective proliferation of RPE cells in the periphery in in vivo studies in pigs. Invest Ophthalmol Vis Sci 48(1):355–360. doi:10.1167/iovs.05-1565
17. Kiilgaard JF, Scherfig E, Prause JU, la Cour M (2012) Transplantation of amniotic membrane to the subretinal space in pigs. Stem Cells Int 2012:716968. doi:10.1155/2012/716968
18. Kyhn MV, Kiilgaard JF, Lopez AG, Scherfig E, Prause JU, la Cour M (2008) Functional implications of short-term retinal detachment

in porcine eyes: study by multifocal electroretinography. Acta Ophthalmol 86(1):18–25. doi:10.1111/j.1600-0420.2007.00983.x

19. Li SY, Yin ZQ, Chen SJ, Chen LF, Liu Y (2009) Rescue from light-induced retinal degeneration by human fetal retinal transplantation in minipigs. Curr Eye Res 34(7):523–535
20. Maaijwee KJ, van Meurs JC, Kirchhof B, Mooij CM, Fischer JH, Mackiewicz J, Kobuch K, Joussen AM (2007) Histological evidence for revascularisation of an autologous retinal pigment epithelium–choroid graft in the pig. Br J Ophthalmol 91(4):546–550. doi:10.1136/bjo.2006.103259
21. Warfvinge K, Kiilgaard JF, Klassen H, Zamiri P, Scherfig E, Streilein W, Prause JU, Young MJ (2006) Retinal progenitor cell xenografts to the pig retina: immunological reactions. Cell Transplant 15(7):603–612
22. Binder S, Krebs I, Hilgers RD, Abri A, Stolba U, Assadoulina A, Kellner L, Stanzel BV, Jahn C, Feichtinger H (2004) Outcome of transplantation of autologous retinal pigment epithelium in age-related macular degeneration: a prospective trial. Invest Ophthalmol Vis Sci 45(11):4151–4160. doi:10.1167/iovs.04-0118
23. Joussen AM, Heussen FM, Joeres S, Llacer H, Prinz B, Rohrschneider K, Maaijwee KJ, van Meurs J, Kirchhof B (2006) Autologous translocation of the choroid and retinal pigment epithelium in age-related macular degeneration. Am J Ophthalmol 142(1):17–30. doi:10.1016/j.ajo.2006.01.090
24. van Meurs JC, Van Den Biesen PR (2003) Autologous retinal pigment epithelium and choroid translocation in patients with exudative age-related macular degeneration: short-term follow-up. Am J Ophthalmol 136(4):688–695
25. Treumer F, Bunse A, Klatt C, Roider J (2007) Autologous retinal pigment epithelium-choroid sheet transplantation in age-related macular degeneration: morphological and functional results. Br J Ophthalmol 91(3):349–353. doi:10.1136/bjo.2006.102152
26. Szurman P, Roters S, Grisanti S, Aisenbrey S, Schraermeyer U, Luke M, Bartz-Schmidt KU, Thumann G (2006) Ultrastructural changes after artificial retinal detachment with modified retinal adhesion. Invest Ophthalmol Vis Sci 47(11):4983–4989. doi:10.1167/iovs.06-0491
27. Christiansen AT, Tao SL, Smith M, Wnek GE, Prause JU, Young MJ, Klassen H, Kaplan HJ, la Cour M, Kiilgaard JF (2012) Subretinal implantation of electrospun, short nanowire, and smooth poly(epsilon-caprolactone) scaffolds to the subretinal space of porcine eyes. Stem Cells Int 2012:454295. doi:10.1155/2012/454295
28. Nazari H, Zhang L, Zhu D, Chader GJ, Falabella P, Stefanini F, Rowland T, Clegg DO, Kashani AH, Hinton DR, Humayun MS (2015) Stem cell based therapies for age-related macular degeneration: the promises and the challenges. Prog Retin Eye Res 48:1–39. doi:10.1016/j.preteyeres.2015.06.004
29. Tezel TH, Del Priore LV, Kaplan HJ (2004) Reengineering of aged Bruch's membrane to enhance retinal pigment epithelium repopulation. Invest Ophthalmol Vis Sci 45(9):3337–3348. doi:10.1167/iovs.04-0193
30. Gullapalli VK, Sugino IK, Van Patten Y, Shah S, Zarbin MA (2005) Impaired RPE survival on aged submacular human Bruch's membrane. Exp Eye Res 80(2):235–248. doi:10.1016/j.exer.2004.09.006
31. Phillips SJ, Sadda SR, Tso MO, Humayan MS, de Juan E Jr, Binder S (2003) Autologous transplantation of retinal pigment epithelium after mechanical debridement of Bruch's membrane. Curr Eye Res 26(2):81–88
32. Hillenkamp J, Hussain AA, Jackson TL, Cunningham JR, Marshall J (2004) The influence of path length and matrix components on ageing characteristics of transport between the choroid and the outer retina. Invest Ophthalmol Vis Sci 45(5):1493–1498
33. Pauleikhoff D, Loffert D, Spital G, Radermacher M, Dohrmann J, Lommatzsch A, Bird AC (2002) Pigment epithelial detachment in the elderly. Clinical differentiation, natural course and pathogenetic implications. Graefes Arch Clin Exp Ophthalmol 240(7):533–538. doi:10.1007/s00417-002-0505-8
34. Ahir A, Guo L, Hussain AA, Marshall J (2002) Expression of metalloproteinases from human retinal pigment epithelial cells and their effects on the hydraulic conductivity of Bruch's membrane. Invest Ophthalmol Vis Sci 43(2):458–465
35. Falabella P, Koss MJ, Stefanini FR, Pfister M, Chader GJ, Thomas BB, Thomas P, Clegg DO, Hinton DR, Humayun MS (2014) Safety outcome of subretinal human embryonic stem cell-derived pigment epithelium (hESC-RPE) transplantation in Yucatan mini-pigs with oral or intravenous immunosupression. Invest Ophthalmol Vis Sci 55(13):2674
36. Swindle MM, Makin A, Herron AJ, Clubb FJ Jr, Frazier KS (2012) Swine as models in biomedical research and toxicology testing. Vet Pathol 49(2):344–356. doi:10.1177/0300985811402846